IEEE Access
Multidisciplinary | Rapid Review | Open Access Journal

Received December 20, 2019, accepted February 7, 2020, date of publication February 24, 2020, date of current version March 6, 2020.

Digital Object Identifier 10.1109/ACCESS.2020.2975985

The Role of Neural Networks in Predicting the Thermal Life of Electrical Machines

GULRUKH TURABEE[1], MUHAMMAD RAZA KHOWJA[2], PAOLO GIANGRANDE[2], (Senior Member, IEEE), VINCENZO MADONNA[2], (Member, IEEE), GEORGINA COSMA[3], (Member, IEEE), GAURANG VAKIL[2], (Member, IEEE), CHRIS GERADA[2,3], (Senior Member, IEEE), AND MICHAEL GALEA[2,4], (Senior Member, IEEE)

[1]School of Science and Technology, Nottingham Trent University, Nottingham NG11 8NS, U.K.
[2]Power Electronics, Machines, and Control Research Group, University of Nottingham, Nottingham NG7 2RD, U.K.
[3]Department of Computer Science, School of Science, Loughborough University, Loughborough LE11 3TU, U.K.
[4]Key Laboratory of More Electric Aircraft Technology of Zhejiang Province, Ningbo 315100, China

Corresponding author: Gulrukh Turabee (gulrukh.turabee@gmail.com)

ABSTRACT For a continuous mode of operation, insulating material in an electrical machine is subject to constant thermal, electrical, mechanical and environmental stresses where thermal stress is a major cause of gradual insulation deterioration, which leads to ultimate winding failure. To guarantee a satisfactory lifetime, electrical machines are designed to operate winding temperatures well below their thermal class, which results in an oversized design. Standard methods for thermal lifetime evaluation of electrical machines are based on accelerated aging tests that require several months of testing. This paper proposes an alternative approach relying on a supervised neural network that significantly shortens the time demanded by accelerated aging tests for thermal lifetime evaluation of electrical machines. The supervised neural network is based on a feedforward neural network trained with Bayesian Regularisation Backpropagation (BRP) algorithm. The network predicts the wire insulation resistance with respect to its aging time at aging temperatures of 250°C, 270°C and 290°C, which reveals a good match of prediction outcomes against the experimental findings. The mean time-to-failure at each aging temperature is extracted using the Weibull probability plot in order to compare the Arrhenius curves for both conventional and proposed method and a relative error of 0.125% is achieved in terms of their temperature indexes. In addition, the analysis shows a time saving of 1680 hours (57% time saved of experimental test procedure) when the thermal life of the insulating material is predicted using BRP neural network.

INDEX TERMS Neural network, aging time, thermal life of insulation, accelerated lifetime test.

I. INTRODUCTION

Many different stresses degrade the life of the insulation system in an electrical machine. In general, there are thermal, electrical, ambient, and mechanical stresses, the so-called ''TEAM'' stresses [1]. Amongst all, thermal stress is the most recognised cause of gradual insulation deterioration resulting in ultimate winding failure. Hence, a winding insulation system must be evaluated for its capability under thermal stress [2], [3]. The operating temperature of a winding is the main cause of the thermal stress, which results from Joule losses plus additional heating due to core eddy currents and hysteresis losses [4], [5]. In insulating materials, this high temperature accelerates chemical reactions involved in the insulation deterioration. This, in turn, leads to the insulation progressively losing its dielectric properties [1], [6]. Insulation lifetime models, based on the Arrhenius laws, are suitable for evaluating the lifetime consumption of electrical machines operating with the continuous-duty cycle, where the winding temperature is mostly constant throughout the working period. According to the Arrhenius law, every 8-10°C rise in temperature reduces the insulation thermal life by halve [7]–[9]. In terms of insulation, the weakest component is represented by the turn-to-turn enamel layer. Indeed, insulation-related failures are generally originated by a turn-to-turn breakdown [10], which yields to over-temperatures

The associate editor coordinating the review of this manuscript and approving it for publication was Saeid Nahavandi.

This work is licensed under a Creative Commons Attribution 4.0 License. For more information, see http://creativecommons.org/licenses/by/4.0/

that can trigger most severe failures (e.g. phase-to-ground short-circuits) and eventually lead to the machine failure.

Traditionally, during the design phase of an electrical machine, the maximum hot-spot temperature that the insulation system can withstand is evaluated using thermal modelling techniques, such as lumped parameters thermal networks (LPTNs), computational fluid dynamics and finite element simulations [5], [11], [12]. The designer, then, acts on the design parameters so that the hot-spot temperature always remains below the thermal class of the adopted insulation [13], [14], which is provided by the manufacturer. This ensures that the electrical machine will survive at least 20,000 hours of continuous operation [15]. To determine the thermal class (or temperature index) of the insulation system, technical standards are available and suggest methodologies for the thermal qualification of the insulation system. This allows for quite accurate estimations of the thermal lifetime at various operating temperatures [16], however, these qualification strategies require extensive testing, which is long-lasting and can endure up to thousands of hours [17]. This paper proposes a neural network to predict the trend of the insulation resistance under thermal aging that estimates the time-to-failure of each specimen at considered aging temperatures. The proposed approach employs the supervised feedforward neural network trained with Bayesian Regularisation Backpropagation (BRP) for the thermal qualification of electrical machine that reduces the experimental time of thermal aging tests while reaching good predictive accuracy. The predicted results from the neural network are validated and compared with the experimental measurements in order to evaluate the effectiveness of the proposed methodology.

II. NEURAL NETWORKS FOR PREDICTING PROPERTIES OF INSULATING MATERIAL

In this section, related work on Artificial Neural Networks (ANNs) which have been proposed to predict the properties of insulating materials is reviewed. In [18], [19], an ANN approach was proposed for the prediction of non-linear properties variations of transformer oil, known as 'BORAK22' and it was used by "SONELGAZ", an electric and gas company. In the study, a supervised ANN, known as Radial Basis Function Gaussian (RBFN) coupled with the Random Optimization Method (ROM) and two learning strategies, namely data adaptive learning and batch learning technique, were used. The dielectric loss of the transformer oil with respect to aging time was predicted with a good agreement between measurements and estimations for both the two learning techniques. In [20], RBFN was tested with different training algorithm of Levenberg-Marquardt (LM) and Back Propagation (BP) for the prediction of aging time of thermal oil. BP prediction results were better as compared to LM ones. Furthermore, the same ANN methods were applied in [21] to predict the tensile strength and breakdown voltage of paper and oil insulation with respect to its aging time. Similarly, after experimenting with various neural networks, RBFN with ROM was chosen for the prediction of breakdown voltage in a point-barrier-plane Air Gap [22], [23]. To acquire better quality prediction results, each time a future value was predicted, the first value was omitted from the training set having the form (Y_i, Y_{i+1}). The results obtained were quite promising with predicted values coherent with experimental values. In [20], [21], the mechanical properties of XLPE cable (Cross-linked Polyethylene) under thermal aging stress, was then predicted through the same use of the aforementioned methods [24], [25]. As a result, the mean value (all specimens) of both tensile strength and elongation at each aging temperature were predicted. Amongst all temperatures, the maximum relative error was 16.1% with ROM and 24.2% with BP. During this analysis, the thermal life of the XLPE cable and its temperature index were also evaluated. An ANN was developed [26] for monitoring and diagnosis of capacitive equipment. The neural network was selected for the prediction of dielectric loss angle, where inputs as voltage, current, capacitance, ambient temperature, humidity and dielectric loss were taken. Since the number of neurons greatly influence the prediction quality, the best performance was reached with 15 neurons. The ANN was able to deliver accurate dielectric loss angle values, whose information allowed to prevent the insulation fault in high-voltage electrical equipment. Shpreker *et al.* [27] proposed a deep learning neural network (i.e. Recurrent Neural Network) to predict insulation resistance of electrical equipment, which yields the early detection against the potential damage of the insulation whilst taken into account variations in external factor such as humidity and air temperature. Long Short-Term Memory (LSTM), a newly developed Recurrent Neural Network (RNN) known for its capability of preserving internal memory, was used for this purpose [18], [19].

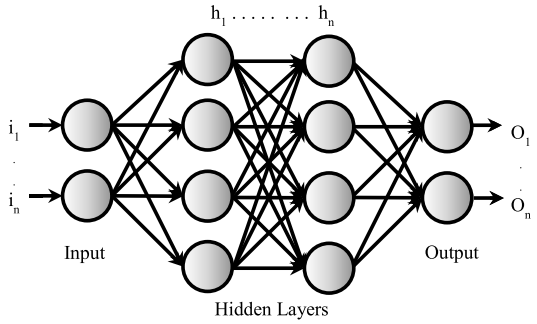

FIGURE 1. General architecture of the neural network.

III. ARCHITECTURE OF THE NEURAL NETWORKS

In general, a typical ANN architecture contains three to four layers known as the input, one or two hidden layers and output, as depicted in Fig. 1. On the first layer, independent variables are given as input, whereas the hidden layers calculate the weights to explore the input effects on the predicted dependent variables through an activation function. On the output layer, the predicted value is presented with associated estimation error [28], [29].

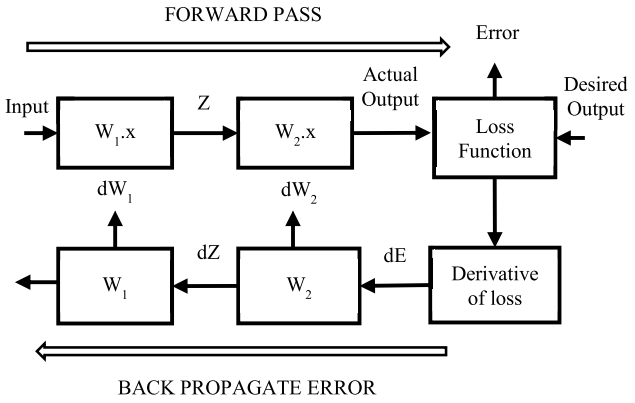

FIGURE 2. Neural Network architecture of BRP & FITNET.

For each input ($i_1 \ldots i_n$, where n is an integer number), let ($w_1 \ldots w_n$) be adjustable weights and let b be an adaptable bias value calculated at the given hidden layer, then they are combined and added. Consequently, a sigmoid activation function Y(Z) is applied to generate an output (2).

$$Y(Z) = \left(1 + e^{-u}\right)^{-1} \tag{1}$$

$$u = \Sigma_j w_j x_j + b \tag{2}$$

In (1), e is the exponential term and u is derived from (2) where b is the bias, w.x is the dot product of w, and x is a vector consisting of the inputs. To predict the life of insulating material, the following neural networks are considered, the architecture of each is explained in sub-sections III.A-III.D. Each neural network discussed was trained using the collected experimental data (i.e. insulation resistance measurements) and the one delivering the best results is selected for the purpose of the presented study.

A. BAYESIAN REGULARISATION BACKPROPAGATION (BRP)

BRP uses the basic feedforward network structure to train the given data. Input values are propagated back and forth (forward and backward pass) from the hidden layer to minimize the relative absolute error and weights values and bias are updated at every propagation [30], as illustrated in Fig. 2. One of the issues that occur during the training of these networks is overfitting in which untrained data when presented to network tends to produce a large error as compared to trained data with small error [31]. In order to overcome this issue, a BRP is employed and its bias and weights are updated by a Levenberg-Marquardt (LM) optimization method. This helps the network to generalise well and minimize the error [31], [32]. For the sample data, if ((X_i, Y_i), (X_N, Y_N)) is the set of input-output pairs in the network, then the parameter of primary interest is weight w_{ij}^k at node j in layer l_k and node i in layer l_{k-1}, and b_i^k is the bias for node i in layer l_k. The error E(X, P) at this point can be calculated between the target and predicted value for a particular value of parameter P. With respect to weights and biases ($w_{ij}^k b_i^k$), the error function is required to be calculated when training the BP neural network using Bayesian RRegularisation. At learning rate α, each time weight and biases are updated denoted P according to:

$$P^{t+1} = P^t - \alpha \frac{\partial E\left(X, P^t\right)}{\partial P} \tag{3}$$

where P^t is the parameter of a Neural Network at iteration t in Bayesian Regularization. Bayesian Regularisation uses the Jacobian for calculations, which gives performance only in terms of mean or sum of squared errors [31]. The performance p in accordance with weights and bias variable x using the Jacobian jj and j_e can be estimated relying on (4) and (5):

$$jj = jx * jx, j_e = j * E \tag{4}$$

$$dY = \frac{-(jj + Q * mu)}{j_e} \tag{5}$$

where Q is the identity matrix and E stands for all errors with mu as the adaptive value. Training is completed when the following conditions are met:

- Performance reached to the goal;
- Maximum number of epochs reached;
- Time is exceeded.

B. FUNCTION FITTING NEURAL NETWORK (FITNET)

FITNET is another commonly used Multi-Layer Perceptron (MLP) or feedforward model containing one hidden layer. The network is mostly adopted for the regression problem [33], which also uses back propagation as its training function (Fig. 2). Given input data with N hidden layers, it returns a network with N+1 layers. Initially, the size of input and output are set as zero and get adjusted during the training phase based on the given training set of data. The default training algorithm for this type of neural network is Levenberg-Marquardt which enables the forecast of future values [34]. The main benefit of using FITNET and BRP is a simple structure, strong reliability and an excellent tool for modeling complex systems [31], [32].

C. LONG SHORT-TERM MEMORY (LSTM)

LSTM, as shown in Fig. 3, acquires the capability of preserving internal memory and learns temporal data on the sequence of upcoming inputs. The major benefit of using LSTM is that long term dependencies can be learned throughout the training and exploited for regression and classification purposes [35]. LSTM is a type of RNN that has been highly widespread because of its improved memory and ability to preserve temporary information [35], [36]. LSTM comprises of special cells known as 'memory blocks' within its hidden layer with self-connections to store the temporary state of network with special multiplicative units as 'gates' to control the flow of information. Within each memory block, the input gate looks over the flow of input activations going in the memory cell whereas the output gate looks over the flow of cell activations to the remaining network [36]. Given an input ($Y = Y_1 \ldots Y_N$), an LSTM network creates a mapping to an

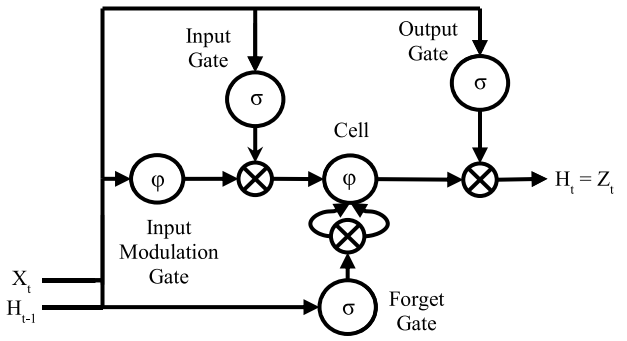

FIGURE 3. Neural Network architecture of RNN.

output data ($Z = Z_1 \ldots Z_N$) by estimating activations using the following equations N times:

$$I_t = \sigma(W_i[h_{t-1} + X_t] + b_i \quad (6)$$
$$f_t = \sigma(W_f[h_{t-1} + X_t] + b_t \quad (7)$$
$$c_t = \tanh(W_c[h_{t-1} + X_t] + b_c \quad (8)$$
$$o_t = \sigma(w_o[h_{t-1} + X_t] + b_o \quad (9)$$
$$h_t = o_t * tanh(c_t) \quad (10)$$

where I_t represents input gate, f_t as forgot gate, c_t as input modulation, o_t as output gate and h_t as hidden state equation with "w" as weight matrices (w_i, w_f, w_c as weight matrices for peephole connections), b represents biases (b_i, b_t, b_c and b_o as input gate bias, forget gate bias, input modulation gate bias and output gate bias respectively).

D. RADIAL BASIS FUNCTION NETWORK (RBFN)

Radial basis in its simplest form is a three-layer feedforward neural network, as shown in Fig. 4, which takes the input of the N-dimensional vector and presents it to Radial Function Function Network (RBFN) that stores a prototype vector [24], [25]. A Gaussian function is used as an activation function to facilitate the training and improve generalisation. The output layer is linear and serves as a summation unit [37]. The concept behind RBF is that to generate output, neuron process the input signal using an activation function for an input x:

$$g(x) = e^{-\frac{(x-\mu)^2}{\sigma^2}} \quad (11)$$

where g(x) gives the output of Gaussian node with mean μ and σ standard deviation. Gaussian neural nodes partition the entire feature vector space generating a signal against an input vector. Distance between the center and the input vector defines the strength of the neuron signal [38]. The advantage of using RBFN are strong tolerance to input noise and fast learning ability [24].

IV. EXPERIMENTAL TEST SETUP

A. TEST SPECIMEN

The test specimen is a twisted pair wire (round enameled magnet wire) with a thermal class of 220°C, wire diameter

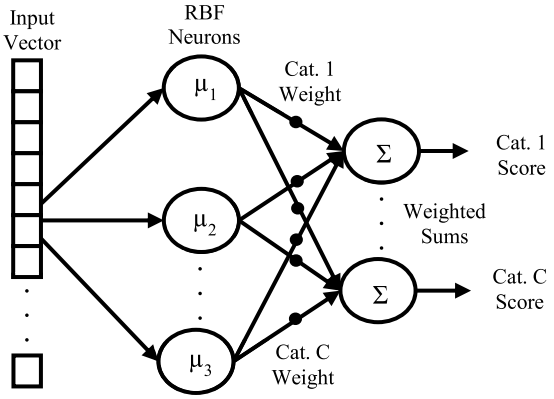

FIGURE 4. Neural Network architecture of RBF Neuron.

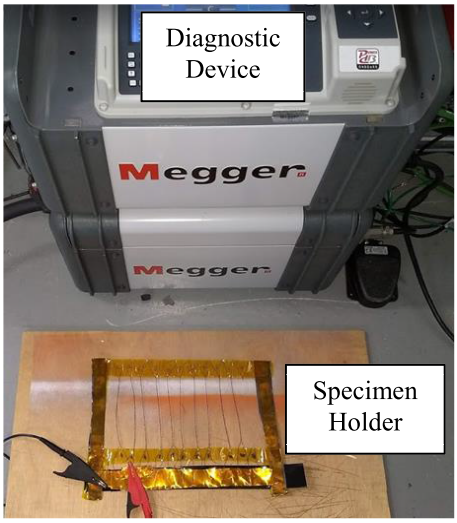

FIGURE 5. Test specimens and MEGGER 4000 diagnostic device.

of 0.4mm and insulation thickness of 22.5μm, as shown in Fig 5. The magnet wire features a double enamel layer, namely a modified-polyester on a base coat and over coated by polyamide-imide. The length of the specimen wire is 200mm with 20 twists on it. The chosen specimen's arrangement is done according to the ASTM standards D2307 [15] since it is aimed for a low voltage electrical machine [39].

B. TEST PROCEDURE

The test procedure is based on the accelerated aging tests, which are commonly used for thermal qualification of insulating material. In such tests, the specimens are thermally aged above the insulation thermal class. A number of 10 twisted pair specimens were considered at three different aging temperatures according to the ASTM D2307 standards. The aging process is carried out in a controlled oven at 250°C, 270°C and 290°C with their corresponding aging cycle of 120h, 48h and 8h respectively. The oven used is "MEMMERT UF260 plus ventilated oven" that can control inside temperature up to 300°C. Prior to the thermal aging procedure, the test specimens were subject to the diagnostic

tests. The diagnostic parameters, such as the dissipation factor (Tanδ), insulation capacitance (IC) and insulation resistance (IR), were measured using MEGGER 4000 at the end of each aging cycle. After every thermal exposure, the cooling time was awaited before the specimens were removed from the oven, and their turn-to-turn diagnosis was assessed using the AC hipot test. This test consists of ramping-up the 50 Hz, the sinusoidal voltage from 0 to 500V_{rms}. When a specimen fails the AC hipot test, the time-to-failure was noted. The aging procedure was carried out until the insulation breakdown is detected on all the specimens.

V. CHOICES AND CONSIDERATIONS

A. SELECTION OF NEURAL NETWORK

The selection of a neural network is finalised in this section, which is taken forward to predict the thermal life of the insulation. The IR measurements of a random specimen (S9) aged at 290 °C were chosen for training the neural networks as discussed in section III with the aim of predicting the IR values. Details on the prediction approaches and an optimum number of neurons are discussed in sections VI-A and V-B respectively. Fig. 6a shows the findings obtained from various neural networks against the measured IR, while the corresponding relative errors are illustrated in Fig. 6b. It can be observed that the FITNET network is having the highest error amongst all. Consequently, BRP has the lowest error below 10% at all aging cycles, therefore, the BRP network was chosen for the prediction analysis of the diagnostic parameters in the next sections. Fig. 7a and Fig. 7b depict the regression plots of actual versus predicted data (Fig. 6) for two neural networks: BRP and FITNET respectively. For both neural networks, the correlation coefficient "R", which quantifies the curve fit goodness, was estimated and the values of 0.9992 and 0.758 were respectively determined for BRP and FITNET (best and worst case). A correlation coefficient close to one indicates that the output has tracked the target value well enough for training hence, the prediction well matches the measurement.

B. INFLUENCE OF CHANGING NEURONS

The performance of the neural network is greatly influenced by the selection of hidden layers and the number of neurons. For the neural network selected from the previous section, only one hidden layer is chosen since the network BRP with one hidden layer in combination with various neurons is enough to predict any finite input-output mapping problem [26]. This makes the prediction results dependent on the number of neurons selected. In order to check the best outcome, the sensitivity analysis was carried out (on IR predicted by BRP in Fig. 6), where the number of neurons was varied from 3 to 50 in step of 1. It was observed that the prediction results were adversely affected when neurons were increased. Fig. 8 reports the relative error against the number of neurons (3 to 10) at aging temperature of 290°C, for a randomly chosen specimen (S9). As can be seen from

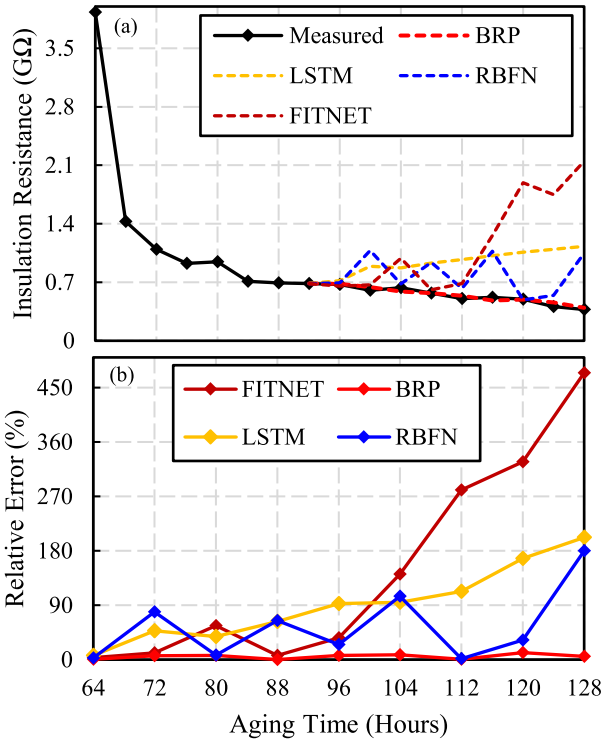

FIGURE 6. Selection of Neural Network. (a) Prediction Result. (b) Relative Error.

Fig. 8, the best performance outcome is achieved at 5 neurons and therefore, it was chosen for the prediction of diagnostic parameters (Tanδ, ΔIC and IR) in the next sub-section.

C. DIAGNOSTIC PARAMETER SELECTION

Using MEGGER 4000, diagnostic parameters such as Tanδ, IC and IR were predicted for a random specimen (S1), aged at 290°C. Fig. 9 shows prediction results of Tanδ, differential IC (ΔIC) and IR using BRP neural network with respect to aging time. The ΔIC is computed using (12), where IC_{500} is the IC measured at 500V and IC_{100} is the IC measured at 100V [40], [41]. As can be observed from Fig. 9, the BRP gives the closest results of IR against the measured data as compared to the diagnostic parameters %ΔIC and Tanδ due to their inconsistent trend. Therefore, IR is chosen as a diagnostic parameter because its prediction reveals a lower mismatch with the actual measurements.

$$\%\Delta IC = 100 \times \frac{IC_{500} - IC_{100}}{IC_{500}} \tag{12}$$

VI. PREDICTION ANALYSIS AND DISCUSSION

For prediction analysis, the accelerated aging test campaign was started and completed at highest aging temperature (i.e. 290°C thermal exposure) until a breakdown in each specimen was detected, in order to set the end of life criterion for other aging temperatures. The test campaign continued for 250°C and 270°C aging temperatures until the 7^{th} aging cycle, where the test procedure was deliberately stopped to predict the life of each specimen using neural network approach. Once the prediction phase was completed,

TABLE 1. IR of each specimen for setting the end of life criterion.

SPECIMEN #	S1	S2	S3	S4	S5	S6	S7	S8	S9	S10	$\%IR_{break}$
%IR	89.50	89.68	89.97	87.38	89.59	81.49	81.90	86.22	90.49	85.93	87.22

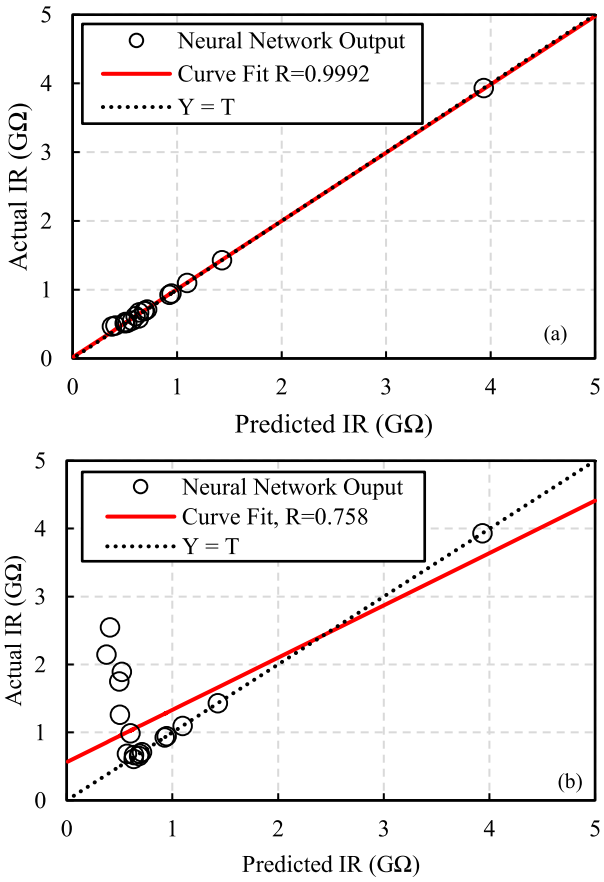

FIGURE 7. Regression Plot of Fig. 6 (a) BRP (b) FITNET.

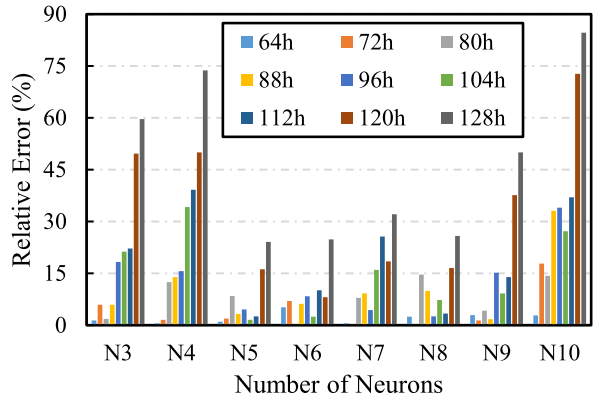

FIGURE 8. Sensitivity Analysis on Number of Neurons.

the experimental test campaign was resumed and completed at 250°C and 270°C aging temperatures (from 8th aging cycle until the insulation failure is detected in each specimen), in order to compare the predicted time-to-failure against the

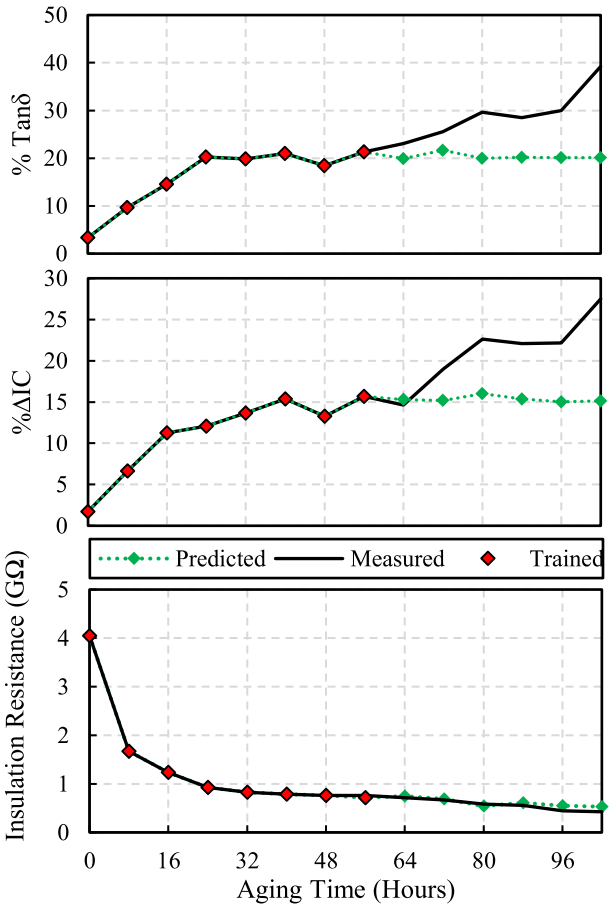

FIGURE 9. Selection of Diagnostic Parameter (290°C Aging Temperature, Sample S1).

actual experimental findings (i.e. for prediction validation purposes).

A. END OF LIFE CRITERION

To obtain an end of life criterion, the percentage insulation resistance (%IR) corresponding to the failure time of each specimen, was determined at the aging temperature of 290°C. The %IR was calculated with respect to its unaged value of each twisted pair specimen using (13), where IR_{end} is the insulation resistance at aging time one cycle before the specimen is failed and IR_{unaged} is the insulation resistance when the specimen is not exposed to the aging temperatures. It was found that, for all 10 specimens, the % IR was in the range of 82% to 90%. Table 1 lists the values of the % IR determined on the 10 specimens where the average ($\%IR_{break}$ = 87.22%) among all the specimens was chosen as the end of life criterion in determining the thermal life of

the insulation.

$$\%IR = 100 \times \frac{IR_{unaged} - IR_{end}}{IR_{unaged}} \tag{13}$$

B. TRAINING AND PREDICTION PHASES

1) TRAINING PHASE

As stated earlier, to train the neural network, the BRP algorithm is used. The training is performed on a given set of specimens (10 per aging temperature) having the form of (X_i, X_{i+1}) where X_i is the value of IR at aging time t_i whereas, X_{i+1} is the predicted value of IR at aging time t_{i+1}.

2) PREDICTION PHASE

For each specimen, to predict the future value of any diagnostic parameter X_{i+1}, where (i = 1,2,3,4....n) at a particular aging time t_{i+1}, the training is performed on a set of data having the input parameter (aging time as (t_i, t_{i+1})) and output parameter (any diagnostic parameter as (X_i, X_{i+1})). The training is repeated from the beginning of each specimen. In order to achieve optimised prediction results, training trade-off exercise is carried out using the BRP training algorithm, based on the selection of a number of learning points (or measurements) used at the training stage.

C. TRAINING TRADE-OFF EXERCISE

This subsection describes different training strategies applied to the dataset in order to train data using the BRP algorithm that depends on various factors to obtain the best prediction outcomes. As stated in [24], the number of learning points to train the network plays a vital role in the learning process of the algorithm and hence, influences the prediction results. Thus, the dataset was investigated with a different number of data points included at the training stage and prediction accuracies were reported. For a given dataset of specimen S9, it was observed that if the training is performed until aging time of 48h and 56h and the rest of the data points is kept for validation of neural network then the percentage error between the actual and predicted values was minimum as compared to the results obtained with other learning times (i.e. below 48h and 56h). The combination of 8 data points (until 56h) for training with 5 neurons (chosen in the previous section) presented the best results so far, however, the prediction results were still not convincing and therefore, the training strategy on the latest predicted data value was adopted. So the training was performed in the loop with the prediction of future value at a time (loop method). The loop was repeated until the last value of the dataset was predicted. With the dataset $(X_i \ldots X_n)$, the network was trained until 56h (8th value) learning time for predicting the future value X_{i+1} (9th value). However, in order to get the X_{i+2} (10th value), the latest predicted value X_{i+1} (9th value) was included in the dataset $(X_i \ldots X_{i+1})$. At the same time, each future value was predicted, the first value of the dataset was omitted. In this way, the training algorithm was not influenced by the previous values (omitted values) of the dataset and hence, the network was fed through an equal number of data points, as depicted in Fig. 10b. With this method, the MAE of 0.032 and RMSE of 0.043 is achieved which is the lowest error when compared to the all other methods previously discussed in this sub-section.

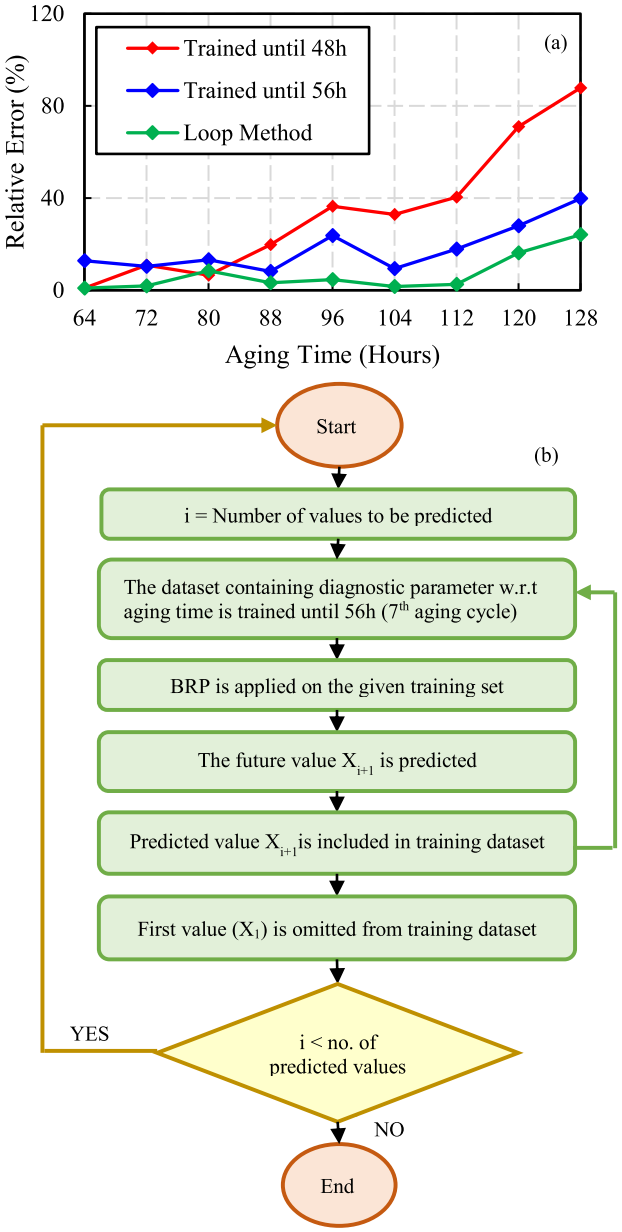

FIGURE 10. Prediction Approach. (a) Comparison of Prediction Methods using BRP. (b) Flow chart of Loop Method.

D. PREDICTION RESULTS

IR of each specimen was predicted using the loop method as discussed in the previous sub-section. The BRP neural network was trained until the 7th aging cycle (to save the time from 7^{th} aging cycle until all the specimens are failed) and the specimens whose failure was detected before the 7th aging cycle were discarded and hence, not included in the neural

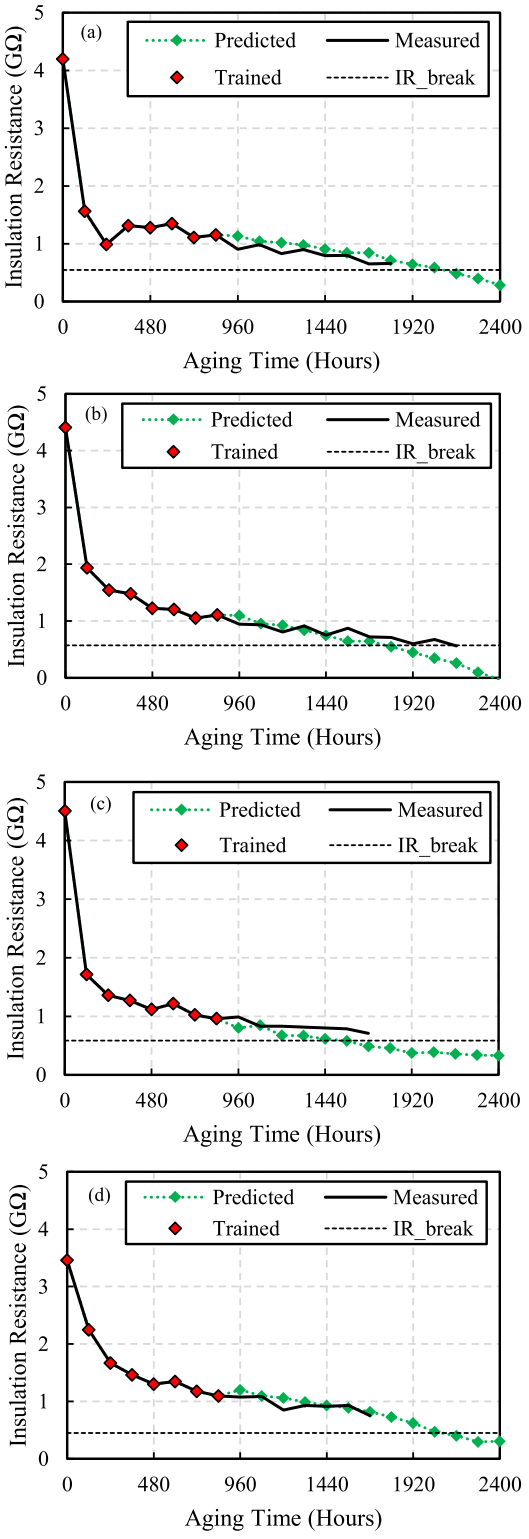

FIGURE 11. Predicted Results at 250°C aging temperature (a) S4 (b) S3 (c) S8 (d) S10.

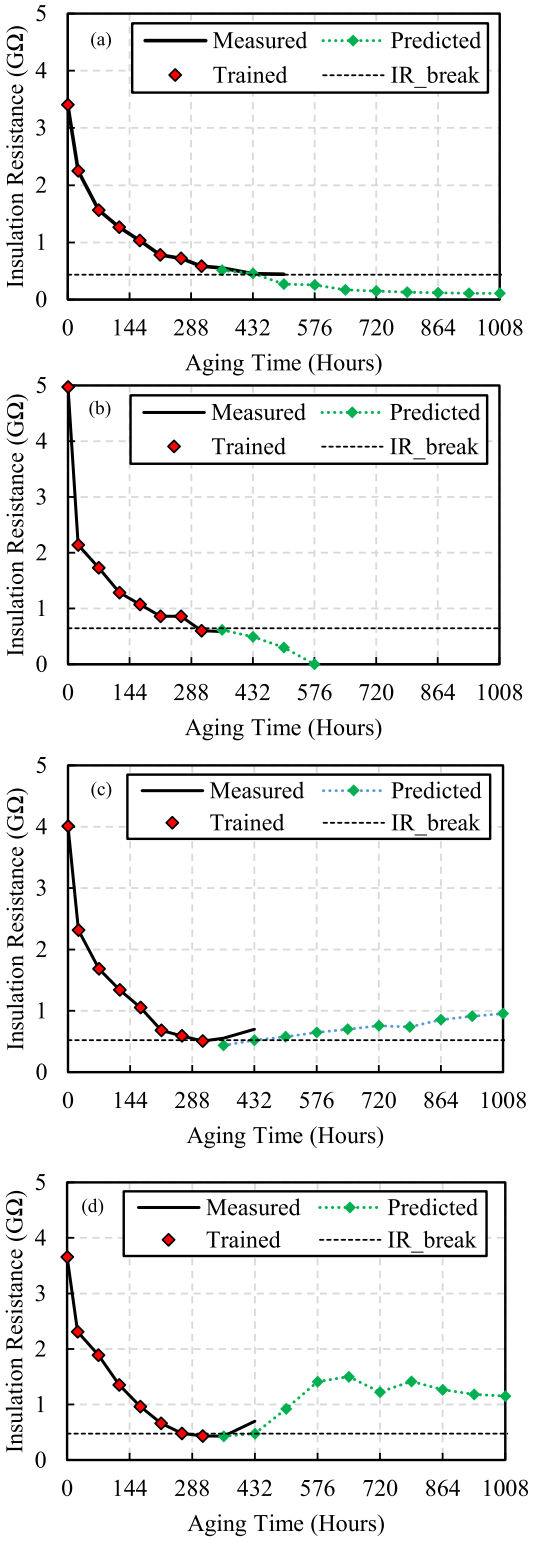

FIGURE 12. Predicted Results at 270°C aging temperature (a) S1 (b) S2 (c) S4 (d) S6.

network for prediction. 8, 9 and 10 number of specimens were survived (total 27 specimens) at 250°C, 270°C and 290°C aging temperatures respectively. To determine the mean time-to-failure of each specimen at different aging temperatures, the neural network was programmed to predict IR for a longer time span (i.e. 2400h, 1008h and 128h at 250°C, 270°C and 290°C aging temperatures respectively) to reach the IR end of life criterion. Fig. 11 to Fig. 13 illustrate the predicted results

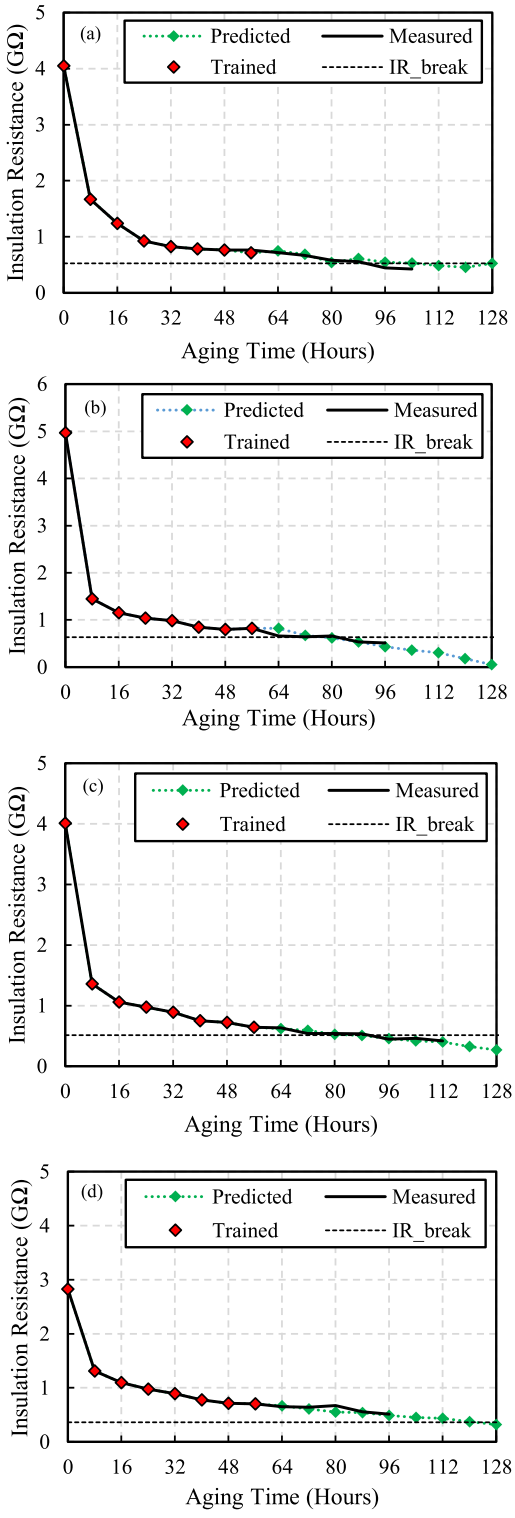

FIGURE 13. Predicted Results at 290°C aging temperature (a) S1 (b) S2 (c) S5 (d) S7.

for the longer period of aging time, where 4 specimens of each aging temperature are shown (although all 27 specimens were predicted using the neural network). The black line is the data measured experimentally (which was resumed and completed after being stopped at 7th aging cycle), red diamonds

TABLE 2. Time-to-failure of each specimen in hour.

SPECIMEN NUMBER	T_1 = 250°C		T_2 = 270 °C		T_3 = 290 °C	
	CM	PM	CM	PM	CM	PM
S1	1740	1875	528	476	108	110
S2	1980	1708	384	383	100	82
S3	2220	1806.9	192	192	116	117.3
S4	1860	2294	456	332	124	118
S5	660	660	456	381	116	86
S6	1140	792.2	340	296	84	127.1
S7	900	1543.6	336	309.2	100	123
S8	1740	1620	336	360	116	119
S9	900	900	288	288.9	132	116
S10	1980	2227	288	321.4	68	94
CM = Conventional Method			PM = Proposed Method			

TABLE 3. Comparison of mean time-to-failure.

AGING TEMPERATURE	250°C	270°C	290°C
Conventional Method	1517.9h	363.7h	108.3h
Proposed Method	1544.2h	337.3h	111.3h
Relative Error (%)	1.73	7.27	2.77

shows the results during the training process, green dotted line is the predicted trend and the black dashed line shows the breakdown value of IR. The specimen is subject to face the breakdown as the predicted value crosses the black dotted line. As can be observed from Fig. 11 to Fig 13, for few specimens, the breakdown using neural network occurs before the actual breakdown of the specimen since the end of life criteria was set at 87.22% reduction in the IR from its associated unaged value. Therefore, the predicted time-to-failures were recorded for each specimen according to the given end of life criteria. For the conventional method, the time-to-failure of a specimen is calculated as the total thermal exposure hours minus half the duration of the aging cycle (the end of life is assumed to occur at half of the last thermal cycle). However, for the neural network method, the time-to-failure is the time duration at which the end of life criteria is reached plus half duration of the aging cycle. The time-to-failure of each specimen is shown in Table 2. It was noticed that the IR of 3 specimens out of 30 have not crossed the breakdown criteria, therefore, the time-to-failure (underlined) of these 3 specimens is considered as the time-to-failure of the specimens obtained from the conventional method. This is done to meet the ASTM standard requirement for insulation lifetime evaluation, which recommends considering at least 10 specimens per thermal exposure. Once the time-to-failure of each specimen was recorded, all the specimens at each aging temperature were plotted on the Weibull probability plot with a 95% confidence interval as shown in Fig. 14a - Fig. 14c. From Weibull distribution plots, the mean time-to-failure is extracted at each aging temperature for both conventional (least mean square method) regression method and proposed neural network method. The mean time-to-failure at each aging temperature is reported in Table 3 along with its associated relative error. Table 3 shows the insulation lifetime from both the methods which comes from the

TABLE 4. Lifetime calculations for conventional method.

	Temperature in C	Temperature in K	X = 1/T	X-square	Life (h)	Y = Log_{10}L	XY = (Log_{10}L)/T	Y-square
1	250	523	1.912e-3	3.655e-6	1517.9	3.18	6.08	10.12
2	270	543	1.842 e-3	3.391e-6	363.7	2.56	4.72	6.56
3	290	563	1.776 e-3	3.154e-6	108.3	2.03	3.61	4.14
N = 3			ΣX = 5.53e-3	ΣX^2 = 1.02e-6		ΣY = 7.78	ΣXY = 14.41	ΣY^2 = 20.82

TABLE 5. Lifetime calculations for proposed method.

	Temperature in C	Temperature in K	X = 1/T	X-square	Life (h)	Y = Log_{10}L	XY = (Log_{10}L)/T	Y-square
1	250	523	1.912e-3	3.655e-6	1544.2	3.19	6.10	10.17
2	270	543	1.842e-3	3.391e-6	337.3	2.53	4.66	6.39
3	290	563	1.776e-3	3.154e-6	111.3	2.05	3.63	4.19
N = 3			ΣX = 5.53e-3	ΣX^2 = 1.02e-6		ΣY = 7.76	ΣXY = 14.39	ΣY^2 = 20.75

50% cumulative probability failure. It can be observed that the lifetime of the insulation predicted by the neural network is very close to the one obtained from the experimental campaign. From the obtained results, the maximum error is 7.27% in the case of 270°C aging temperature whereas, the minimum error of 1.73% is achieved at 250°C aging temperature which shows the effectiveness of the proposed method in terms of shortening the test campaign for the accelerated aging tests. Hence, a considerable amount of testing time can be saved, since only 8 experimental diagnostic cycles are necessary to train the neural network, whether or not breakdown is detected in all the specimens.

VII. LIFETIME MODEL AND ARRHENIUS PLOT

For accelerated thermal aging, the deterioration process is a first-order chemical reaction in which the rate of the reaction is defined by the Arrhenius law, which was proposed by Dakin in 1971 [1]–[3], [7]. Based on the Arrhenius law, the thermal life of solid insulation is given by:

$$L = Ae^{B/T} \tag{14}$$

where, A and B are insulation constants, which are determined by the experimental data while L is the insulation life in hours at operating temperature T in Kelvin. The life of the insulation (14) can be expressed as a linear function by taking log on both sides as:

$$log_{10}L = \log_{10} A + (log_{10}e).\frac{B}{T} \tag{15}$$

By looking at (15), the life of insulation represents an equation of straight line with B' as the slope of the line and A' as the y-intercept. Hence, (15) can be written in the form:

$$Y = A'X + B' \tag{16}$$

where: $Y = \log_{10}L$
$A' = \log_{10}A$
$X = 1/T$
$B' = (\log_{10}e).\ B$

TABLE 6. Constants and temperature index.

PARAMETERS	A'	B'	T.I (°C)	R
Conventional Method	-12.97	8445.2	215.85	0.9997
Proposed Method	-12.93	8420.4	215.58	0.9976
Relative Error (%)	0.31	0.29	0.125	0.21

With the help of least square method, the constants A' and B' are derived using the data obtained from both the experimental campaign and the proposed neural network as:

$$A' = \frac{\sum Y - B' \sum X}{N} \tag{17}$$

$$B' = \frac{N \sum XY - \sum X \sum Y}{N \sum X^2 - (\sum X)^2} \tag{18}$$

where N is the number of aging temperatures tested Using (16), the temperature index at 20,000h insulation life can be calculated as in (19):

$$Temperature\ Index = \frac{B'}{4.301 - A'} - 273 \tag{19}$$

The correlation coefficient R is determined relying on (20):

$$R = \sqrt{\frac{A' \sum Y + B' \sum XY - N(Y_{avg})^2}{\sum Y^2 - N(Y_{avg})^2}} \tag{20}$$

Using Table 4, Table 5 and equations (16) to (19), the constants A' and B', the temperature index and the correlation coefficient are calculated for both the conventional method and proposed method which are reported in Table 5. In Fig. 15, an Arrhenius curve is plotted i.e. the thermal life of insulation is extrapolated to a lifetime of 20,000h using the constants given in Table 5. The lifetime points fits the equation of a straight line with correlation coefficient very close to unity, which shows the curve fit goodness of insulation life using both conventional and proposed method. The obtained relative error of temperature index is 0.125% when comparing insulation's lifetime using conventional method with the proposed method. The advantage of saving time using the proposed method is quite clear. Time that has

TABLE 7. Time comparison of conventional and proposed method.

AGING TEMPERATURE	250°C	270°C	290°C	TOTAL
Conventional Method	2280h	552h	136h	2968h
Proposed Method	840h	312h	136h	1288h
Network Time Elapse	0.115h	0.13h	0.144h	0.388h
Time Saving	1440h	264h	0h	≈1680h

been saved using the proposed method is 1440h and 264h at aging temperature of 250°C and 270°C respectively which saved 1680h (70 days) in total as illustrated in Table 6. Table 7 shows the thermal exposure time comparison between the conventional and proposed methods of insulation lifetime evaluation. The time saving is estimated from a specimen that lasted the longest minus the time at which the neural network was trained. For example, specimen S3 lasted the longest at 250°C thermal exposure, failed at the 2280h aging time while the neural network was trained at 7th aging cycle (i.e. 840h aging time) which gives the time saving of 1440h. Similarly, for 270°C thermal exposure, specimen S1 lasted the longest, failed at 552h while the neural network was trained at 312h aging time, giving the time saving of 264h. The time elapsed for the neural network for each specimen is calculated as 51.82 seconds using the "toc" command in MATLAB. The total time elapsed for the survived specimens at each aging temperature is illustrated in Table 7. For the purpose of comparison, the time elapse is converted into hour that took about 0.388h (23.3mins), to predict total of 27 survived specimens in the experimental test campaign, which is negligible when compared with the time-savings using proposed method and hence, neglected in the time saving analysis.

VIII. PRACTICAL CONSIDERATIONS

The proposed method, a Bayesian Regularized Artificial Neural Network, discussed in the previous sections verified with the experimental results was able to reduce the accelerated aging test procedure time by approximately 57% compared to conventional method of insulation's lifetime evaluation, without any significant compromise on lifetime accuracy. However, the proposed method requires to be adopted in line with certain considerations to appropriately implementing the proposed prediction method using a neural network.

A. PRE-CONDITIONING PROCESS

Prior to the accelerated aging tests, a set of specimens at each thermal exposure was subjected to a pre-conditioning process. The specimen was pre-conditioned for 12 hours' time, equal to the insulation thermal class of the enameled magnet wire (i.e. 220°C in the present case), in order to minimise the extrinsic thermal aging due to pre-conditioning itself. This pre-conditioning process is very important as the momentary high thermal exposure removes any volatile moisture and substances from the layer of dielectric insulation. These impurities can significantly influence the measurement

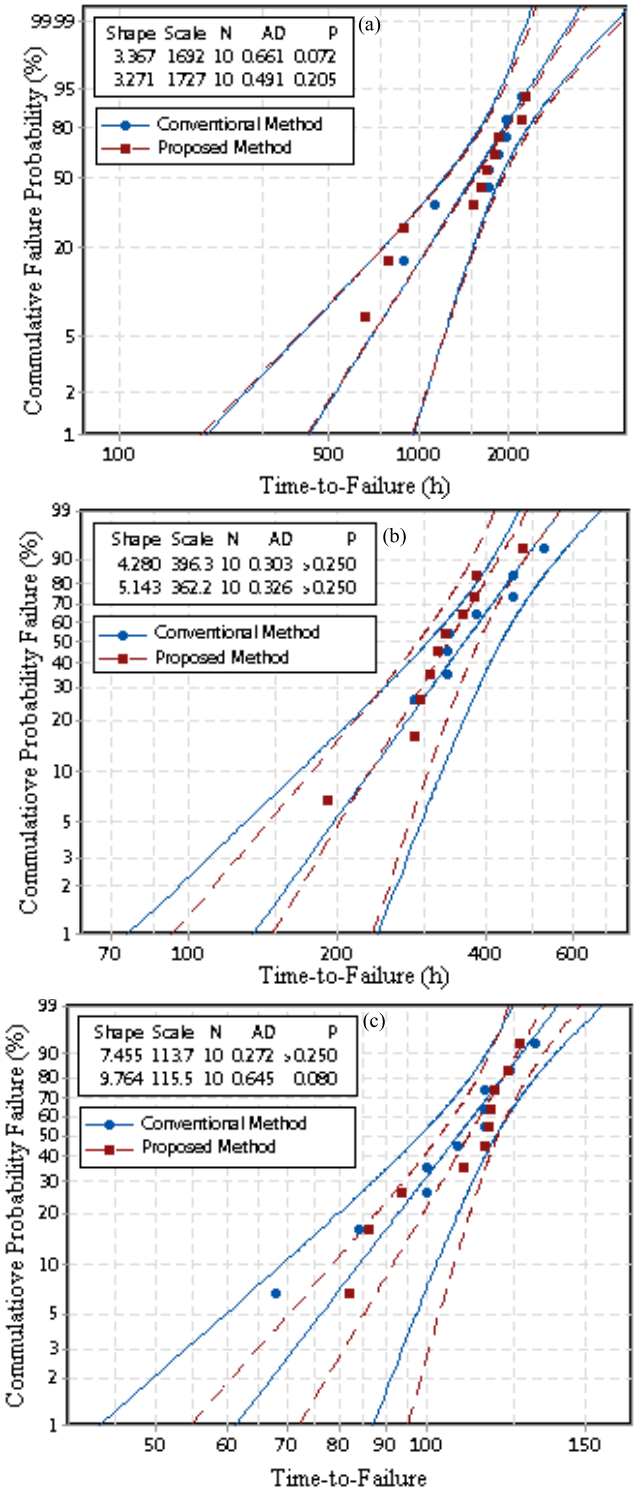

FIGURE 14. Weibull Probability Plot (a) 250°C (b) 270°C (c) 290°C.

of the dielectric properties [42] that can result in a collection of data with high variability. For this reason, the 'unaged' term in the presented study is referred to a pre-conditioned specimen, since the specimen is still unaged (i.e. 0h) at this point of time.

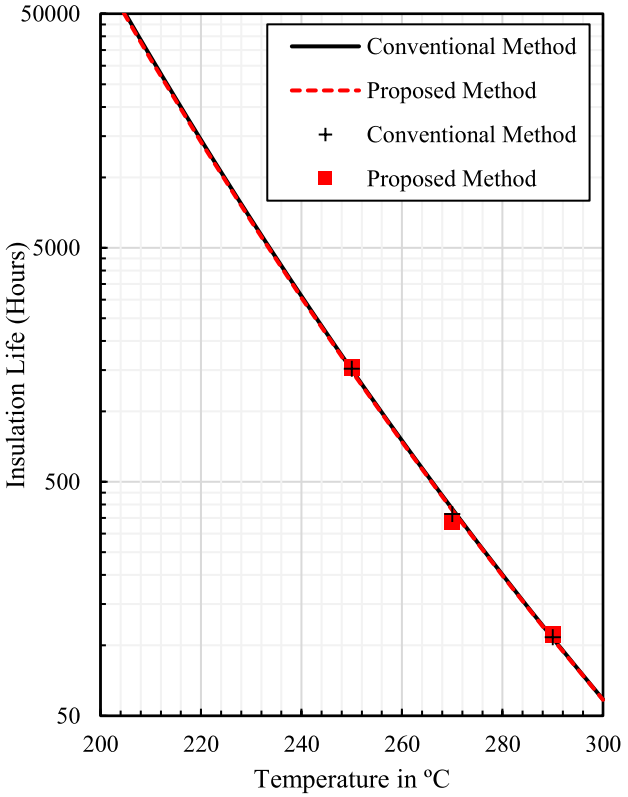

FIGURE 15. Arrhenius Plot using conventional and proposed method.

B. ENVIRONMENTAL FACTORS

Environmental factors, such as ambient temperature and relative humidity, also play a vital role in the measurement process of the diagnostic properties [43]. Thus, the diagnostic cycles must be carried out in a controlled environment i.e. ambient temperature and relative humidity is monitored, for leveling out the effect of the environmental factors on the diagnostic parameters [41]. The diagnostic tests, carried out in the presented study, were performed below the ambient temperature of 25°C and relative humidity of 40%, after being removed from the oven.

C. THERMAL EXPOSURE TIME AND LEARNING TIME

Thermal exposure time for each aging cycle was selected according to the rule described by Arrhenius law which states that every 8-10°C rise in temperature reduces the insulation thermal life by half [7]–[9]. To enhance the statistical significance of the predicted time-to-failure, the number of aging cycles must be considered between 10 and 20 as recommended in [44]. The thermal exposure time can be obtained using (21), where T_i is the aging temperature considered during the test procedure, T_o is the insulation thermal class, k is the number of desired aging cycles and 20,000 represents the life of insulation at thermal class defined by the manufacturer.

$$T_{exp} = \frac{20,000 \times 2^{(T_0 - T_i)/10}}{k} \tag{21}$$

Based on (21), the exposure times of 120h, 48h and 8h were obtained for the aging temperature of 250°C, 270°C and 290°C respectively. For the neural network method of predicting the insulation' lifetime, it is always best to have more data points (aging cycles) so that more data can be trained until the chosen learning time, leading to a more accurate prediction of the diagnostic parameters. This can be seen in Fig. 9, where the trend of ΔIC and Tanδ is not monotonic that results in an inaccurate prediction outcome.

To get the utmost benefit out of the proposed method, accelerated aging test must be completed at the shortest accelerated aging point (i.e. the highest aging temperature), in order to set an end of life criterion for all the aging temperatures. Prediction analysis showed that the obtained end of life criterion (Table 1) was reasonable for all the considered aging temperatures, despite 3 specimens were failed at a very early age. In order to meet the requirement of ASTM standards (i.e. at least 10 specimens at each aging temperature), additional specimens (for example 15 at each aging temperature) may be considered prior to commencing the test campaign. In this way, specimens failing at early age (i.e. not enough points to train the network) can be excluded from the prediction analysis using neural network. Unlike 290°C aging temperature, for other aging temperatures, only few diagnostic sessions (aging cycles) were required to train the neural network, hence, the number of performed diagnostic sessions are reduced compared to the one demanded by the conventional method of insulation's lifetime evaluation. In the presented work, it has been shown that 8 data points are enough (until 7th aging cycle) to train the neural network in order to get the desired IR prediction. However, it is worth looking into an analysis in which the number of aging cycles may be reduced to train the network whilst keeping the same number of data points in the training set. This can either be done by increasing the value of k in (21) at each thermal exposure or by using the data extrapolation methods, which yields to a more time saving of the experimental test campaign.

D. APPLICABILITY

In terms of applicability of the proposed method, the neural network, despite being verified for turn-to-turn polyester/polyamide insulation is suitable for other varieties of organic insulations for electrical machines rated at low voltage levels, including phase-to-ground and phase-to-phase insulation systems. Furthermore, it is worth recalling that the presented work is the case-study of the electrical machine where no varnish or impregnation was applied to the specimens. In circumstances where winding's mechanical protection is prerequisite, the winding of electrical machines is required to be varnished which in principle, does not affect the applicability of the proposed method. Depending on the specific application and the required technology, the electrical machine may still need to be qualified according to technical qualification standards, such as IEC 60034 18-21 and IEEE Std. 117-2015, before entering into the market. The proposed method of thermal lifetime evaluation does not claim to replace these standards which when required, must

be followed by the machine's manufacturers. The presented work is mainly directed toward machine design engineers and researchers since it aims to develop thermal lifetime models, which can be used during the initial stage of prototyping in order to improve the machine's reliability. Thus, a precise idea on the insulation thermal class can be obtained with reduced diagnostic sessions of accelerated thermal aging tests [41].

IX. CONCLUSION

Since aerospace and transportation industries are shifting toward electrified solutions, quicker thermal qualification and hence faster manufacturing of electrical machines are becoming very important. Excellent advances have been made in the last two decades in terms of computationally efficient electromagnetic and thermal analysis of electrical motors. On the other hand, reliability, lifetime evaluation and physics of failure are becoming essential requirements for motor-drive systems. Therefore, these aspects cannot be considered as secondary objectives anymore. In this paper, using the proposed Neural Network (BRP), a faster alternative method was adopted for the thermal qualification of electrical machine, which showed a good quality of prediction when compared to the conventional method of thermal qualification. The proposed network predicted the wire insulation resistance with respect to its aging time at aging temperatures of 250°C, 270°C and 290°C. The mean time-to-failure at each aging temperature was extracted using Weibull probability distribution to compare the Arrhenius curves for both conventional and proposed methods. This gave the error of 0.125% when its temperature indexes were compared. Moreover, the analysis showed a time saving of 1680 hours (57% time saved of accelerated aging test campaign), when the thermal life of insulation is predicted using the BRP neural network, without any major compromise on lifetime accuracy. On the other hand, the time elapsed for the neural network itself took about just 0.388h (23.3mins) in total, in order to predict 27 survived specimens at all aging temperatures.

REFERENCES

[1] G. C. Stone, E. A. Boulter, I. Culbert, and H. Dhirani, *Electrical Insulation for Rotating Machines: Design, Evaluation, Aging, Testing, and Repair* vol. 21. Hoboken, NJ, USA: Wiley, 2004.

[2] V. Madonna, P. Giangrande, L. Lusuardi, A. Cavallini, and M. Galea, "Impact of thermal overload on the insulation aging in short duty cycle motors for aerospace," in *Proc. IEEE Int. Conf. Electr. Syst. Aircr., Railway, Ship Propuls. Road Vehicles Int. Transp. Electrific. Conf. (ESARS-ITEC)*, Nov. 2018, pp. 1–6.

[3] V. Madonna, P. Giangrande, L. Lusuardi, A. Cavallini, C. Gerada, and M. Galea, "Thermal overload and insulation aging of short duty cycle, aerospace motors," *IEEE Trans. Ind. Electron.*, vol. 67, no. 4, pp. 2618–2629, Apr. 2020.

[4] V. Madonna, P. Giangrande, C. Gerada, and M. Galea, "Thermal analysis of fault-tolerant electrical machines for more electric aircraft applications," *J. Eng.*, vol. 2018, no. 13, pp. 461–467, Jan. 2018.

[5] V. Madonna, A. Walker, P. Giangrande, G. Serra, C. Gerada, and M. Galea, "Improved thermal management and analysis for stator end-windings of electrical machines," *IEEE Trans. Ind. Electron.*, vol. 66, no. 7, pp. 5057–5069, Jul. 2019.

[6] M. Farahani, E. Gockenbach, H. Borsi, K. Schafer, and M. Kaufhold, "Behavior of machine insulation systems subjected to accelerated thermal aging test," *IEEE Trans. Dielectr. Electr. Insul.*, vol. 17, no. 5, pp. 1364–1372, Oct. 2010.

[7] T. W. Dakin, "Electrical insulation deterioration treated as a chemical rate phenomenon," *Trans. Amer. Inst. Elect. Eng.*, vol. 67, no. 1, pp. 113–122, Jan. 1948.

[8] V. M. Montsinger, "Loading transformers by temperature," *Trans. Amer. Inst. Electr. Eng.*, vol. 49, no. 2, pp. 776–790, Apr. 1930.

[9] G. C. Montanari and L. Simoni, "Aging phenomenology and modeling," *IEEE Trans. Electr. Insul.*, vol. 28, no. 5, pp. 755–776, Oct. 1993.

[10] S. Grubic, J. M. Aller, B. Lu, and T. G. Habetler, "A survey on testing and monitoring methods for stator insulation systems of low-voltage induction machines focusing on turn insulation problems," *IEEE Trans. Ind. Electron.*, vol. 55, no. 12, pp. 4127–4136, Dec. 2008.

[11] M. Popescu, D. A. Staton, A. Boglietti, A. Cavagnino, D. Hawkins, and J. Goss, "Modern heat extraction systems for power traction machines—A review," *IEEE Trans. Ind. Appl.*, vol. 52, no. 3, pp. 2167–2175, May 2016.

[12] A. Boglietti, A. Cavagnino, D. Staton, M. Shanel, M. Mueller, and C. Mejuto, "Evolution and modern approaches for thermal analysis of electrical machines," *IEEE Trans. Ind. Electron.*, vol. 56, no. 3, pp. 871–882, Mar. 2009.

[13] P. Lindh, I. Petrov, A. Jaatinen-Varri, A. Gronman, M. Martinez-Iturralde, M. Satrustegui, and J. Pyrhonen, "Direct liquid cooling method verified with an axial-flux permanent-magnet traction machine prototype," *IEEE Trans. Ind. Electron.*, vol. 64, no. 8, pp. 6086–6095, Aug. 2017.

[14] V. Madonna, P. Giangrande, A. Walker, and M. Galea, "On the effects of advanced end-winding cooling on the design and performance of electrical machines," in *Proc. 13th Int. Conf. Electr. Mach. (ICEM)*, Sep. 2018, pp. 311–317.

[15] *Standard Test Method for Thermal Endurance of Film-Insulated Round Magnet Wire*, Standard ASTM-D2307, 2013.

[16] *Test Procedure for the Determination of the Temperature Index of enamelled and Tape Wrapped Winding Wires*, Standard IEC 60172, 2015.

[17] P. Mancinelli, S. Stagnitta, and A. Cavallini, "Qualification of hairpin motors insulation for automotive applications," *IEEE Trans. Ind. Appl.*, vol. 53, no. 3, pp. 3110–3118, May 2017.

[18] L. Mokhnache, A. Boubakeur, B. O. Noureddine, M. A. R. Bedja, and A. Feliachi, "Application of neural networks in the thermal ageing prediction of transformer oil," in *Proc. Power Eng. Soc. Summer Meeting. Conf.*, 2001, pp. 1865–1868.

[19] L. Mokhnache, A. Boubakeur, and N. Nait Said, "Application of neural networks paradigms in the diagnosis and thermal ageing prediction of transformer oil," in *Proc. IEEE 14th Int. Conf. Dielectric Liquids. ICDL (Cat. No.02CH9)*, Jul. 2002, pp. 258–261.

[20] L. Mokhnache, A. Boubakeur, and N. N. Said, "Comparison of different neural networks algorithms used in the diagnosis and thermal ageing prediction of transformer oil," in *Proc. IEEE Int. Conf. Syst., Man Cybern.*, vol. 6, Oct. 2002, Art. no. 6.

[21] L. Mokhnache, P. Verma, and A. Boubakeur, "Neural networks in prediction of accelerated thermal ageing effect on oil/paper insulation tensile strength," in *Proc. IEEE Int. Conf. Solid Dielectr. (ICSD)*, vol. 2, Jul. 2004, pp. 575–577 Vol.2.

[22] L. Mokhnache and A. Boubakeur, "Prediction of the breakdown voltage in a point-barrier-plane air gap using neural networks," in *Proc. Annu. Rep. Conf. Electr. Insul. Dielectr. Phenomena*, 2001, pp. 369–372.

[23] L. Mokhnache and A. Boubakeur, "The use of some paradigms of neural networks in prediction of dielectric properties for high voltage liquid solid and gas insulations," in *Proc. Conf. Rec. IEEE Int. Symp. Electr. Insul.*, Apr. 2002, pp. 306–309.

[24] L. Boukezzi and A. Boubakeur, "Prediction of mechanical properties of XLPE cable insulation under thermal aging: Neural network approach," *IEEE Trans. Dielectr. Electr. Insul.*, vol. 20, no. 6, pp. 2125–2134, Dec. 2013.

[25] L. Boukezzi and A. Boubakeur, "Comparison of some neural network algorithms used in prediction of XLPE HV insulation properties under thermal aging," in *Proc. IEEE Int. Conf. Condition Monitor. Diagnosis*, Sep. 2012, pp. 1218–1222.

[26] J.-X. Zhao, H.-Z. Jin, and H.-W. Han, "Dielectric loss factor forecasting based on artificial neural network," in *Proc. 2nd Int. Conf. Inf. Comput. Sci.*, 2009, pp. 177–180.

[27] D. M. Shprekher, G. I. Babokin, and E. B. Kolesnikov, "Application of neural networks for prediction of insulation condition in networks with isolated neutral," in *Proc. Int. Russian Autom. Conf. (RusAutoCon)*, Sep. 2019, pp. 1–6.
[28] T. K. Gupta and K. Raza, "Optimization of ANN Architecture: A Review on Nature-Inspired Techniques," in *Machine Learning in Bio-Signal Analysis and Diagnostic Imaging*. Amsterdam, The Netherlands: Elsevier, 2019, pp. 159–182.
[29] *Artificial Neural Network Model*. Accessed: Dec. 7, 2019. [Online]. Available: https://www.sciencedirect.com/topics/engineering/artificial-neural-network-model
[30] F. Burden and D. Winkler, "Bayesian regularization of neural networks," in *Artificial Neural Networks* (Methods in Molecular Biology), vol. 458, D. J. Livingstone, Ed. Totowa, NJ, USA: Humana Press, 2008.
[31] *MathWorks Documentation—BRP*. Accessed: Dec. 8, 2019. [Online]. Available: https://uk.mathworks.com/help/deeplearning/ref/trainbr.html
[32] Z. Ma, L. Yang, H. Bian, M. S. Bhutta, and P. Xu, "An improved IPM for life estimation of XLPE under DC stress accounting for space-charge effects," *IEEE Access*, vol. 7, pp. 157892–157901, 2019.
[33] J. Buitrago and S. Asfour, "Short-term forecasting of electric loads using nonlinear autoregressive artificial neural networks with exogenous vector inputs," *Energies*, vol. 10, no. 1, p. 40, Jan. 2017.
[34] *MathWorks Documentation—FITNET*. Accessed: Dec. 5, 2019. [Online]. Available: https://ch.mathworks.com/help/deeplearning/ref/fitnet.html
[35] H. Sak, A. Senior, and F. Beaufays, "Long short-term memory recurrent neural network architectures for large scale acoustic modeling," in *Proc. 15th Annu. Conf. Int. Speech Commun. Assoc.*, 2014, pp. 338–342.
[36] R. G. Hefron, B. J. Borghetti, J. C. Christensen, and C. M. S. Kabban, "Deep long short-term memory structures model temporal dependencies improving cognitive workload estimation," *Pattern Recognit. Lett.*, vol. 94, pp. 96–104, Jul. 2017.
[37] E. Kang. (2017). *Long Short-Term Memory (LSTM): Concept*. Accessed: Dec. 10, 2019. [Online]. Available: https://medium.com/@kangeugine/long-short-term-memory-lstm-concept-cb3283934359
[38] S. Khemaissia and M. Morris, "Review of networks and choice of radial basis function networks for system identification," *Technol. Avancées*, vol. 6, pp. 55–85, 1994.
[39] P. Giangrande, V. Madonna, S. Nuzzo, and M. Galea, "Design of fault-tolerant dual three-phase winding PMSM for helicopter landing gear EMA," in *Proc. IEEE Int. Conf. Electr. Syst. Aircr., Railway, Ship Propuls. Road Vehicles Int. Transp. Electrific. Conf. (ESARS-ITEC)*, Nov. 2018, pp. 1–6.
[40] V. Madonna, P. Giangrande, G. Migliazza, G. Buticchi, and M. Galea, "On the thermal insulation qualification of low voltage electrical machines," in *Proc. 45th Annu. Conf. IEEE Ind. Electron. Soc. (IECON)*, Oct. 2019, pp. 7115–7120.
[41] V. Madonna, P. Giangrande, G. Migliazza, G. Buticchi, and M. Galea, "A time-saving approach for the thermal lifetime evaluation of low voltage electrical machines," *IEEE Trans. Ind. Electron.*, to be published.
[42] T. Wakimoto, H. Kojima, and N. Hayakawa, "Measurement and evaluation of partial discharge inception voltage for enameled rectangular wires under AC voltage," *IEEE Trans. Dielectr. Electr. Insul.*, vol. 23, no. 6, pp. 3566–3574, Dec. 2016.
[43] V. Madonna, P. Giangrande, and M. Galea, "Evaluation of strand-to-strand capacitance and dissipation factor in thermally aged enamelled coils for low-voltage electrical machines," *IET Sci., Meas. Technol.*, vol. 13, no. 8, pp. 1170–1177, Oct. 2019.
[44] *IEEE Standard Test Procedure for Thermal Evaluation of Systems of Insulating Materials for Random-Wound AC Electric Machinery*, IEEE Standard 117-2015 (Revision of IEEE Std 117-1974), 2016, pp. 1–34.

GULRUKH TURABEE received the B.S. degree in computer science from the Institute of Business Administration (IBA), Karachi, Pakistan, in 2017, and the Master of Research (MRes) degree in computer science from Nottingham Trent University, U.K., in September 2019. Her research interests are in the field of artificial intelligence and machine learning (including deep learning) applied to the biomedical and electrical engineering applications.

MUHAMMAD RAZA KHOWJA received the B.Eng. degree (Hons.) in electrical power engineering from the Mehran University of Engineering and Technology, Jamshoro, Pakistan, in 2011, the M.Sc. degree in electrical engineering in 2012, and the Ph.D. degree in electrical and electronics engineering from the University of Nottingham, U.K., in 2018. He is currently working as a Research Fellow with the Power Electronics, Machines, and Control (PEMC) Group, University of Nottingham. His main research interests include integrated passive components, design and development of high-performance electrical machines for aerospace applications, and characterization of insulating materials for electrical machine's applications.

PAOLO GIANGRANDE (Senior Member, IEEE) received the bachelor's (Hons.), master's (Hons.), and Ph.D. degrees in electrical engineering from the Politecnico of Bari, Bari, Italy, in 2005, 2008, and 2011, respectively. In 2008, he was a Marie Curie IntraEuropean Fellow with the University of Malta. Since 2012, he has been a Research Fellow with the Power Electronics, Machines and Control Group, University of Nottingham, Nottingham, U.K. Since 2017, he has also been the Head of the Accelerated Lifetime Testing Laboratory, Institute of Aerospace Technology, Nottingham. His main research interests include sensorless control of ac electric drives, design and testing of electromechanical actuators for aerospace, thermal management of high-performance electric drives, and reliability and lifetime modeling of electrical machines.

VINCENZO MADONNA (Member, IEEE) received the B.Sc. degree in electronic engineering from the University of Calabria, Rende, Italy, in 2012, and the M.Sc. degree in electrical engineering from the University of Bologna, Bologna, Italy, in 2016. He is currently pursuing the Ph.D. degree in electrical machines design with the Institute for Aerospace Technology, (IAT), University of Nottingham, Nottingham, U.K. In 2012, he was an Exchange Student with KU Leuven, Belgium. In 2015, he was a Visiting Researcher with the University of Nottingham, where he is also a Marie Curie Fellow with the IAT and the Power Electronics, Machines, and Control (PEMC) Group. His research interests include design, thermal management, and lifetime prediction modeling of electrical machines. He received the qualification of Italian Chartered Engineer, in 2016. He has serves as a Reviewer for the IEEE TRANSACTIONS ON INDUSTRIAL ELECTRONICS, the IEEE TRANSACTIONS ON TRANSPORTATION ELECTRIFICATION, and various IEEE-sponsored International Conferences.

GEORGINA COSMA (Member, IEEE) received the B.Sc. degree (Hons.) in computer science from Coventry University, U.K., in 2003, and the Ph.D. degree in computer science from the University of Warwick, U.K., in 2008. She is currently a Senior Lecturer/Associate Professor with the Department of Computer Science, Loughborough University, U.K. Her research interests focus on data science, deep learning, computational intelligence, nature-inspired feature selection, and feature engineering. She is a member of various IEEE communities, including the IEEE Computer Society, the IEEE Computational Intelligence Society, Big Data Community, Brain Community, Cloud Computing Community, the Internet of Things Community, and Smart Cities Community. She is also the Principal Investigator of The Leverhulme Trust Project Grant entitled Novel Approaches for Constructing Optimized Multimodal Data Spaces (RPG-2016-252).

GAURANG VAKIL (Member, IEEE) received the Ph.D. degree in variable speed generator design for renewable energy applications from the Power Electronics, Machines, and Drives Group, Indian Institute of Technology Delhi, New Delhi, India, in 2016. He subsequently worked as a Research Associate with the Power Electronics, Machines, and Controls Group, University of Nottingham, Nottingham, U.K., where he was appointed as an Assistant Professor with the Electrical and Electronics Engineering Department, in 2016. His main research interests include design and development of high-performance electrical machines for transport and propulsion, optimizing electric drive-train for pure electric and hybrid vehicles (aerospace and automotive), high-power density machines, and magnetic material characterization.

CHRIS GERADA (Senior Member, IEEE) received the Ph.D. degree in numerical modeling of electrical machines from the University of Nottingham, Nottingham, U.K., in 2005. He subsequently worked as a Researcher with the University of Nottingham, on high-performance electrical drives and on the design and modeling of electromagnetic actuators for aerospace applications. Since 2006, he has been the Project Manager of the GE Aviation Strategic Partnership. In 2008, he was appointed as a Lecturer of electrical machines, in 2011, as an Associate Professor, and in 2013, as a Professor at the University of Nottingham. His main research interests include the design and modeling of high-performance electric drives and machines. He is currently the past Chair of the IEEE IES Electrical Machines Committee. He is also an Associate Editor of the IEEE TRANSACTIONS ON INDUSTRY APPLICATIONS.

MICHAEL GALEA (Senior Member, IEEE) received the Ph.D. degree in electrical machines design from the University of Nottingham, Nottingham, U.K., in 2013. He was appointed as a Lecturer, an Associate Professor, and a Professor of electrical machines and drives with the University of Nottingham, in 2014, 2018, and 2019, respectively. He is currently the Head of the School of Aerospace, University of Nottingham Ningbo China, where he is also the Director of Aerospace. He also lectures in electrical machines and drives and in aerospace systems integration and manages a number of diverse projects and programs related to the more/all electric aircraft, electrified propulsion, and associated fields. His main research interests include design and development of electrical machines and drives (classical and unconventional), reliability and lifetime degradation of electrical machines, and the more electric aircraft. He is a Fellow of the Royal Aeronautical Society. He is also on the Executive Board of the U.K., Magnetics Society.